

20.1% Efficient Silicon Solar Cell With Aluminum Back Surface Field

Tobias Fellmeth, S. Mack, J. Bartsch, D. Erath, U. Jäger, R. Preu, F. Clement, and D. Biro

Abstract—We present a standard p⁺pn⁺ solar cell device exhibiting a full-area aluminum back surface field (BSF) and a conversion efficiency of 20.1%. The front side features a shallow emitter which has been exposed to a short oxidation step and reduces the emitter dark saturation current density j_{oe} to 160 fA/cm² on a textured surface. The front contact is formed by light-induced nickel and silver plating. Also, devices featuring screen-printed front contacts have been realized that reach a conversion efficiency of 19.8%. PC1D simulations are presented in order to extract the electronic parameters of the BSF. Therefore, external quantum efficiency and reflectance have been determined for modeling the internal quantum efficiency by adapting surface recombination and lifetime of the PC1D-simulated silicon device. As a result, a recombination velocity of $S_{BSF} = 283$ cm/s and a dark saturation current density of $j_{BSF} = 274$ fA/cm² in the Al BSF are determined. This results in an effective diffusion length $L_{eff} = 1150$ μm.

Index Terms—Al back surface field (BSF), light-induced plating (LIP), screen printing, silicon solar cell.

I. INTRODUCTION

THE ALUMINUM alloyed screen-printed (SP) and fired rear contact is still the most common approach for providing the p-contact for industrial p-type silicon solar cells. This is due, on the one hand, to the cost-effective process sequence featuring screen printing and contact firing and, on the other hand, to its reliability and simplicity. In the past, several authors presented progress in the conversion efficiency of Al-BSF devices. Schulz *et al.* [1] report 18.7% efficient silicon solar cells on 2 × 2 cm² float zone (FZ) material. So does Hilali *et al.* [2] on comparable material by reaching 19%. In 2010, Hörteis *et al.* [3] present 19.3% efficiency by utilizing a more advanced metal jet printing technique followed by light-induced plating (LIP). However, in this letter, we present a solar cell with conversion efficiency exceeding 20% that features a full-area Al BSF on a 1-Ω · cm FZ-Si substrate and a cell size of 2 × 2 cm².

II. EXPERIMENTAL

A cross section of the device is shown in Fig. 1. The front side features an emitter with a sheet resistance of ~80 Ω/sq.

Manuscript received April 15, 2011; revised May 11, 2011; accepted May 16, 2011. Date of publication June 20, 2011; date of current version July 27, 2011. The review of this letter was arranged by Editor P. K.-L. Yu.

The authors are with the Fraunhofer ISE, 79110 Freiburg, Germany (e-mail: tobias.fellmeth@ise.fraunhofer.de; Sebastian.Mack@ise.fhg.de; jonas.bartsch@ise.fhg.de; Denis.Erath@ise.fhg.de; ulrich.jaeger@ise.fhg.de; ralf.preu@ise.fhg.de; Florian.clement@ise.fhg.de; Daniel.biro@ise.fhg.de).

Color versions of one or more of the figures in this letter are available online at <http://ieeexplore.ieee.org>.

Digital Object Identifier 10.1109/LED.2011.2157656

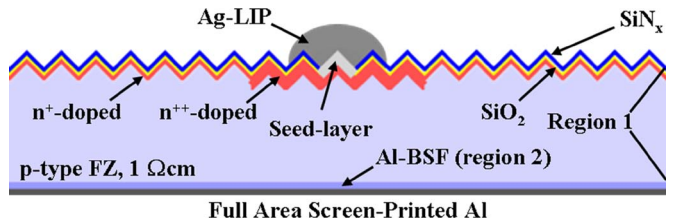


Fig. 1. Representative for the solar cells presented, the cross section of the “Ni-LIP-seed-Ag-LIP device” is scheduled. (Thickness $W = 225$ μm). The device is separated in regions for PC1D simulations.

After a conventional POCl₃ diffusion, the phosphorus silicate glass is heated locally by a laser where the metal front contacts will later be located. Thus, phosphorus in the glass is additionally incorporated into the silicon, forming a highly n-doped region (n⁺⁺) that is called a selective emitter [4].

By applying a short thermal oxidation step at 840 °C, a 10-nm-thick SiO₂ layer is grown on both sides of the device. Due to the additional thermal budget, the surface concentration of phosphorus decreases due to diffusion into the silicon. This approach is very similar to the TOPAS concept, which was presented in detail by Mack *et al.* [5]. The passivation of highly n⁺-doped silicon by SiO₂ is more effective than that by SiN_x [6]. A λ/4 layer of amorphous plasma-enhanced-chemical-vapor-deposited SiN_x : H is segregated on top of the SiO₂, reducing reflectivity and providing the essential hydrogenation of the Si–SiO₂ interface.

By ink-jet printing an etch resist mask on the front with openings for the contacts and dipping the cell into buffered hydrofluoric acid, the dielectric layer is opened, exposing the n⁺⁺-doped emitter. Screen printing of an Al layer on the rear and subsequent firing in a conveyor belt furnace with industrial-type belt speeds form the rear p-contact. The thin SiO₂ layer on the rear is resolved during firing and hence does not retard the BSF formation. Nickel is deposited by LIP where the openings in the dielectric layers have been etched. Forming gas anneal at 400 °C forms a Ni silicide, providing the mechanical and electric contact. By applying a LIP step [7], silver is deposited, forming the bulk finger generating a line resistivity of the metal grid of 2 μΩ · cm.

III. RESULTS

In Table I, the *IV* parameters of the solar cells processed within this work are shown. Three different front metallization techniques were applied. The most advanced approach features a Ni seed layer and a silver-plated finger grid reaching a conversion efficiency of 20.1%, which we believe is the highest value

TABLE I
MEASURED IV PARAMETERS AT STANDARD TESTING CONDITIONS IN DEPENDENCE ON THE FRONT METALLIZATION. THE FRONT END OF THE PROCESS REMAINS UNCHANGED. ALL RESULTS WERE INDEPENDENTLY CONFIRMED BY FRAUNHOFER ISE CALLAB USING SPECTRUM AM 1.5 IEC60904-3ED.2 (2008)

Front Metallization	V_{oc} (mV)	j_{sc} (mA/cm ²)	FF (%)	η (%)
Ni-LIP seed, Ag-LIP	648	38.6	80.6	20.1
SP seed, Ag-LIP	645	37.7	81.3	19.8
SP only	646	37.2	81.8	19.6

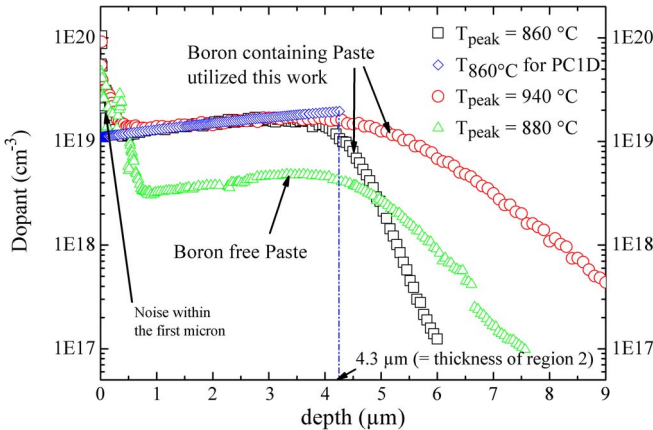


Fig. 2. Three Al profiles measured with the ECV technique. The profiles have been obtained for similar printing quantity belt speed. The $T_{peak} = 860^{\circ}\text{C}$ curve accords to the ECV $T_{peak} = 860^{\circ}\text{C}$ profile how it is employed in PC1D.

reported for solar cells featuring an SP full-area Al alloyed rear contact on a $2 \times 2 \text{ cm}^2$ sized device so far. Due to a seed layer width of $30 \mu\text{m}$ and a final finger width of $50 \mu\text{m}$, an excellent short-circuit current density j_{sc} of 38.6 mA/cm^2 is achieved.

In order to reduce complexity, the Ni contact has been replaced by an SP seed layer incorporating a silver-based paste optimized for providing excellent printability and electrical contact. The lateral conductivity is also provided by Ag LIP. Due to wider fingers ($80\text{--}90 \mu\text{m}$), the fill factor FF is increased, but j_{sc} is decreased compared to the Ni cell; thus, the efficiency η ends up at 19.8%. Within the third approach, the front metallization is only provided by screen printing a standard paste. Still, an efficiency of 19.6% is achieved.

IV. PC1D MODELING

In general, it is observed that the open-circuit voltage V_{oc} reaches high values of nearly 650 mV . That is in the range of rear passivated solar cells [12]. In order to perform a detailed analysis of the results achieved within this work, PC1D modeling [8] was performed, focusing on the V_{oc} .

Electrochemical capacitance-voltage (ECV) measurements provide the Al-BSF profile. Fig. 2 shows two dopant profiles fired at peak temperatures of 860°C and 940°C from the boron-containing paste which has been utilized within this work.

For comparison, a profile of a boron-free paste is displayed, reaching a significant lower dopant level. By extrapolation to $depth = 0 \mu\text{m}$, a curve is obtained, representing the “surface-effect-free” profile in the device. The tail of the ECV profile is

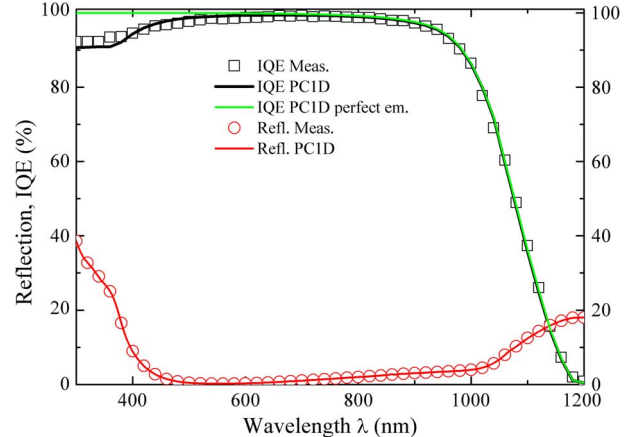


Fig. 3. Reflection and IQE as measured and simulated with PC1D for the Ni-LIP seed cell using the adapted profile shown in Fig. 2. S_{Back} denotes the recombination velocity at the BSF eutectic-layer interface.

TABLE II
PARAMETERS THAT ARE INCORPORATED IN THE PC1D SIMULATION ARE DISPLAYED. REGIONS 1 AND 2 ARE DEFINED ACCORDING TO FIG. 1

Cell	Rear first and subsequent bounce	$n_i(\text{cm}^{-3}) @ 300 \text{ K}$	Region 1	Region 2		
		$\tau_{\text{SRH}} (\mu\text{s})$	$S_{\text{Front}} (\text{cm/s})$	$\tau_{\text{SRH}} (\text{ns})$	$S_{\text{Back}} (\text{cm/s})$	
Ni-LIP seed, Ag LIP	74 %	$9.65*10^9$	10^7	$1.5*10^4$	5.14	10^7
SP seed, Ag-LIP	74 %	$9.65*10^9$	10^7	$1.5*10^4$	5.4	10^7

cut off by continuing linearly in such a way that the amount of dopants accords to the measured curve. This is done exemplarily for the “squared curve,” resulting in the “diamond-shaped” profile applicable for PC1D simulations. The adaptation of the measured ECV profile within this work is motivated and originated by the work done by Huster and Schubert [9]. In Fig. 3, the internal quantum efficiency (IQE), the reflection, and the PC1D simulations from the Ni-LIP seed cell are shown by utilizing the adapted profile shown in Fig. 2. The escape reflection is fitted by adapting the rear reflectance conditions.

In order to provide the most accurate simulation, the bulk is divided into regions 1 and 2 as it is shown in Fig. 1. In region 1, the Shockley–Read–Hall lifetime τ_{SRH} is set to “infinity.” However, in region 2, it is calculated as proposed by Altermatt *et al.* [10], using a parameterization of τ_{SRH} in the presence of the acceptor density N_{ac} in the Al BSF

$$\frac{1}{\tau_{\text{SRH}}} = 2.8339 \cdot 10^{-24} \frac{N_{\text{ac}}}{\text{cm}^{-3}}^{1.5048} \cdot f, \quad " \tau_{\text{SRH}} " = \text{ns} \quad (1)$$

where f denotes a free parameter which is set to $2 \cdot 10^{-6}$. However, this is not valid for our paste, which features boron as an additive. Thus, f needs to be reevaluated in a way that measured and simulated IQEs match. In doing so, we found that, for our paste, $f = 10^{-6}$ fits best that results in an average lifetime in the Al-BSF region 2 as it is shown in Table II.

In order to estimate the V_{oc} limit of the rear side, emitter recombination is set to zero, and hence, the performance is just dominated by the rear.

TABLE III
SPECIFIC CELL PARAMETERS EXTRACTED BY PC1D SIMULATIONS ARE DISPLAYED. j_{0e} IS OBTAINED FROM SYMMETRIC SAMPLES FEATURING THE UTILIZED Emitter. THE UNIT OF V_{oc} AND V_{oc-lim} IS IN MILLIVOLTS

Cell	V_{oc-lim} perf. em.	j_{0b} (fA/cm ²)	L_{eff} (μm)	S_{BSF} (cm/s)	j_{BSF} (fA/cm ²)	V_{oc-lim} $j_{0e}+j_{0b}$	V_{oc} I-V
Ni seed, Ag-LIP	664	230	1150	283	274	650	648
SP seed, Ag-LIP	662	240	1110	299	289	649	645

In Table II, the input parameters that are incorporated in the PC1D simulation are presented. τ_{SRH} is obtained for the “SP seed cell” in analogy to the “Ni-LIP seed cell” by adapting the “circle-shaped curve” in Fig. 2 accordingly to the “diamond-shaped curve” and subsequently using (1).

In Table III, the extracted parameters of the PC1D simulation are shown. In both cases, the rear side limits the V_{oc} to 664 and 662 mV, respectively. The dark saturation current density j_{0b} of the bulk and the rear is calculated with the one-diode model. The effective diffusion length L_{eff} is obtained by [11]

$$L_{eff} = q \cdot D_n \cdot n_i^2 \cdot (j_{0b} \cdot N_{Base})^{-1} \quad (2)$$

where q is the elementary charge, D_n is the minority diffusion coefficient in the base, and N_{Base} is the base doping. The effective recombination velocity of the Al BSF S_{BSF} can be obtained according to [10]

$$S_{BSF} = D_n \cdot \frac{1 - \frac{L_{eff}}{L} \cdot \tanh\left(\frac{W}{L}\right)}{L_{eff} - L \cdot \tanh\left(\frac{W}{L}\right)}. \quad (3)$$

A bulk diffusion length L of 2480 μm is assumed that corresponds to the Auger and radiative limit according to Kerr and Cuevas [12]. Also, the expression for j_{BSF} is given in [11] which is

$$j_{BSF} = q \cdot n_i^2 \cdot S_{BSF} \cdot N_{Base}^{-1}. \quad (4)$$

By extracting the dark saturation current density of the emitter $j_{0e} = 160$ fA/cm² from symmetric samples, the V_{oc} 's of the nonmetallized and metallized cells are obtained, respectively. The V_{oc} accords to the measured value very well if recombination at the metal-emitter interface is considered.

The two results underscore the approach by simulating the Al BSF with PC1D and utilizing (1) by adapting f from $2 \cdot 10^{-6}$ to 10^{-6} . An effective S_{BSF} of 283 cm/s and a j_{BSF} of 274 fA/cm² are achieved, which is an excellent value just for a full-area SP and alloyed Al rear contact.

V. CONCLUSION

A 20.1% efficient silicon solar cell has been presented exhibiting a standard SP aluminum rear p-contact. The front side

features a laser-doped selective emitter which is contacted by Ni silicide. Also, a cell featuring an SP seed layer and a plated finger has been presented reaching an efficiency of 19.8%. By only utilizing the common one-step screen-printing technology, 19.6% could be demonstrated within this work.

All the cells presented feature a high open-circuit voltage of almost 650 mV, which could be explained by the rear Al dopant level, which is nearly one magnitude higher than that of a common profile. PC1D simulations underscore the excellent rear side by separating the rear from the front, showing a $V_{oc-lim} = 664$ mV of the rear side. An effective recombination velocity S_{BSF} of 283 cm/s and a dark saturation current density j_{BSF} of 274 fA/cm² for the Al BSF on 1-Ω · cm FZ-Si are extracted. This also results in a high effective diffusion length of 1150 μm, which exceeds the cell thickness by far with a factor of five.

ACKNOWLEDGMENT

The author would like to thank Prof. Clement, J. Greulich, B. Thaidigsmann, R. Woehl, and M. Glatthaar for fruitful discussions.

REFERENCES

- [1] O. Schulz, A. Mette, M. Hermle, and S. W. Glunz, “Thermal oxidation for crystalline silicon solar cells exceeding 19% efficiency applying industrially feasible process technologies,” *Progr. Photovolt. Res. Appl.*, vol. 16, no. 4, pp. 317–324, Jun. 2008.
- [2] M. M. Hilali, K. Nakayashiki, A. Ebong, and A. Rohatgi, “High-efficiency (19%) screen-printed textured cells on low-resistivity float-zone silicon with high sheet-resistance emitters,” *Progr. Photovolt. Res. Appl.*, vol. 14, no. 2, pp. 135–144, Mar. 2003.
- [3] M. Hörteis, J. Benick, J. Nekarda, A. Richter, R. Preu, and S. W. Glunz, “Fundamental studies on the front contact formation resulting in a 21% efficient silicon solar cell with printed rear and front contacts,” in *Proc. 35th IEEE PVSC*, USA, 2010.
- [4] U. Jäger, M. Okanovic, M. Hörteis, A. Grohe, and R. Preu, “Selective emitter by laser doping from phosphosilicate glass,” in *Proc. 24th EU PVSEC*, Hamburg, Germany, 2009, pp. 1740–1743.
- [5] S. Mack, U. Jäger, A. Wolf, S. Nold, R. Preu, and D. Biro, “Simultaneous front emitter and rear surface passivation by thermal oxidation—An industrially feasible approach to a 19% efficient PERC device,” in *Proc. 25th EU PVSEC*, Valencia, Spain, 2010, pp. 2218–2222.
- [6] M. J. Kerr, J. Schmidt, A. Cuevas, and J. H. Bultman, “Surface recombination velocity of phosphorus silicon solar cell emitters passivated with plasma enhanced chemical vapor deposited silicon nitride and thermal silicon oxide,” *J. Appl. Phys.*, vol. 89, no. 7, pp. 3821–3826, Apr. 2001.
- [7] J. Bartsch, V. Radtke, C. Savio, and S. W. Glunz, “Progress in understanding the current paths and deposition mechanisms of light induced plating and implications for the process,” in *Proc. 24th EU PVSEC*, Hamburg, Germany, 2009, pp. 1469–1474.
- [8] D. A. Clugston and P. A. Basore, “PC1D version 5.32-bit solar cell modeling on personal computers,” in *Proc. 26th IEEE Photovoltaic Spec. Conf.*, Anaheim, 1997, pp. 207–210.
- [9] F. Huster and G. Schubert, “ECV doping profile measurement of aluminum alloyed back surface fields,” in *Proc. 20th EU PVSEC*, Barcelona, Spain, 2005, pp. 1462–1465.
- [10] P. Altermatt, S. Steingrube, Y. Yang, C. Sprodowski, T. Dezhdar, S. Koc, B. Veith, S. Herrman, R. Bock, K. Bothe, J. Schmidt, and R. Brendel, “Highly predictive modeling of entire Si solar cells for industrial applications,” in *Proc. 24th EU PVSEC*, Hamburg, Germany, 2009, pp. 901–906.
- [11] A. L. Fahrenbruch and R. H. Bube, *Fundamentals of Solar Cells*. New York: Academic, 1983.
- [12] M. J. Kerr and A. Cuevas, “General parameterization of auger recombination in crystalline silicon,” *J. Appl. Phys.*, vol. 91, no. 4, pp. 2473–2480, Feb. 2002.